Effect of the repulsive core on the exciton spectrum in a quantum ring

2002 J. Phys.: Condens. Matter 14 73

(http://iopscience.iop.org/0953-8984/14/1/307)

INSTITUTE OF PHYSICS PUBLISHING JOURNAL OF PHYSICS: CONDENSED MATTER

J. Phys.: Condens. Matter **14** (2002) 73–86 PII: S0953-8984(02)27633-X

Effect of the repulsive core on the exciton spectrum in a quantum ring

B Szafran, J Adamowski and S Bednarek

Faculty of Physics and Nuclear Techniques, University of Mining and Metallurgy (AGH), Kraków, Poland

E-mail: bszafran@agh.edu.pl

Received 6 August 2001, in final form 15 October 2001
Published 7 December 2001
Online at stacks.iop.org/JPhysCM/14/73

Abstract

A theoretical study of an exciton confined in a quantum ring is presented. The quantum ring is described as a two-dimensional circular quantum dot with a repulsive core, which is modelled with the help of two Gaussian functions. We have applied the variational method and investigated the evolution of the low-energy exciton spectrum with the change of the confinement potential. The calculations have been performed for the recently produced self-assembled ring-shaped InGaAs quantum dots. We have shown that the repulsive core strongly increases the radiative transition probability from the exciton ground state at the expense of the decreasing probability of the transitions from the excited states. This effect results from the orthogonality properties of the exciton wavefunctions, which are specific to the quantum-ring confinement potential. We have studied the characteristic features of the exciton spectrum, which can be used as a signature of the presence of the repulsive core in the quantum-dot potential.

1. Introduction

In a semiconductor quantum dot, the motion of charge carriers is limited in all the three dimensions to a region of the size of several nanometres [1]. This leads to the three-dimensional quantization of the motion of confined charge carriers, i.e. the energy levels are discrete and the system exhibits the properties similar to a natural atom. For this reason the system of the charge carriers localized in the quantum dot is frequently called an artificial atom [2, 3]. Among various types of quantum dots, the self-assembled quantum dots are the subject of extensive study [4–11] because of their possible applications in optical devices. Recently, it has been shown that—by applying an appropriate growth technique [12–14]—one can obtain self-assembled quantum dots with a ring-like geometry. This discovery along with the capacitance-spectroscopy measurements [12, 13] and the observation of the optical emission

from a charge-tunable structures [14] have inspired several theoretical studies on quantum rings [15–21]. In particular, the magnetic field effects on excitons confined in the quantum rings of finite width have been studied theoretically in [20] and [21]. The authors [20,21] formulated contradictory conclusions concerning a possibility of the observation of the Aharanov–Bohm oscillations for an exciton confined in a quantum ring with finite width. According to the results [20] the interband transition probability for the ground state is much larger than the transition probabilities for the excited states. On the other hand, the authors [21] argued that the oscillator strengths for the ground and excited states are almost equal. We note that the authors of both the papers [20,21] took as a starting point of their concepts the strictly one-dimensional quantum ring [22,23].

In this paper we present a different approach. Namely, we investigate the evolution of the exciton energy spectrum as the shape of the confinement potential changes from a circular quantum dot to a quantum ring when a repulsive core is introduced into the confinement potential. This investigation allows us to understand the qualitative differences between the spectra of the exciton confined in the potential with and without the repulsive core. We describe the characteristic features of the spectra, which can be used in an experimental determination of the presence and the strength of the repulsive core. Moreover, we solve the above-mentioned controversy regarding the relative oscillator strengths for the ground and excited states of the exciton in a quantum ring.

Optical spectra of excitons confined in flat (two-dimensional) quantum dots were studied by Adolph *et al* [24] for quantum disks and by Glutsch *et al* [25] for square quantum dots. Stier *et al* [26] investigated the excitons in pyramid shaped quantum dots. The influence of the exciton and biexciton states on the optical gain in quantum dots with infinitely deep confinement potential was studied by Hu *et al* [27].

In our recent papers [28, 29], we have proposed a Gaussian confinement potential for quantum dots of spherical [28] and cylindrical [29] symmetry. The application [29] of the three-dimensional Gaussian model potential allowed us to reproduce correctly the photoluminescence spectra [11] of isolated and vertically coupled InGaAs self-assembled quantum dots measured with the use of state-filling spectroscopy [30]. In this paper, we modify this model in order to describe the exciton energy spectrum in self-assembled InGaAs quantum rings [12–14]. Here, we adopt an approximation of strictly two-dimensional motion of the charge carriers. In the case of a single charge carrier, the two-dimensional approximation is justified if the height of the nanostructure is much smaller than its lateral size [6]. Then, one can expect that several lowest-energy states of the in-plane motion are associated with the same state of the quantized motion in the growth direction and that the low-energy spectrum is determined mainly by the lateral confinement potential. This condition is well fulfilled for the InGaAs quantum rings [13], which are the subject of the present study. The height of the rings is estimated to be 2 nm, whereas the outer radius is of order of 50 nm. We note, however, that for two or more charge carriers the assumption that the charge density distribution is two-dimensional affects their mutual Coulomb interaction. Nevertheless, we believe that this feature does not change the qualitative effect of the repulsive core on the exciton energy spectrum, which we study in the present paper.

2. Theoretical model

The strain-induced $In_XGa_{1-X}As$ self-assembled quantum dots and quantum rings are in fact islands of locally increased concentration of indium substituting gallium, embedded in the GaAs matrix [31]. We assume that the variation of the effective concentration X of indium in the nanostructure is determined by a smoothly varying function $X(\rho)$ and that the confinement

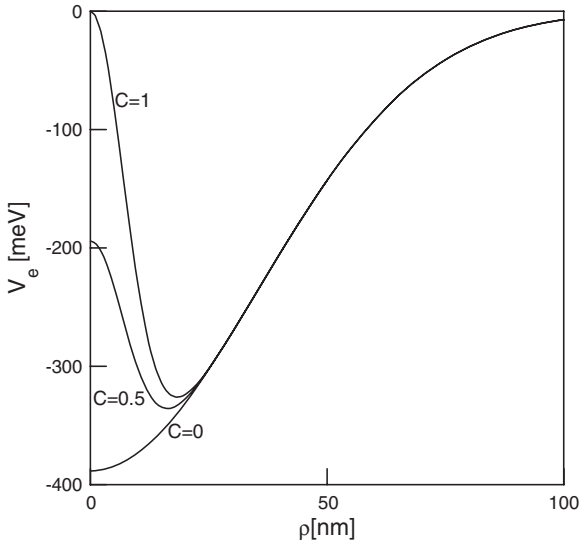

Figure 1. Electron confinement potential V_e for the quantum dot ($C = 0$) and the quantum rings ($C = 0.5$ and 1) as a function of distance ρ from the centre of the nanostructure.

potentials are given by [29]

$$V_e(\rho) = -0.7\ \Delta E_g\ X(\rho) \tag{1}$$

for the electrons and

$$V_h(\rho) = -0.3\ \Delta E_g\ X(\rho) \tag{2}$$

for the holes, where $\Delta E_g = 1.11$ eV is the band gap difference between GaAs and InAs. According to recent measurements [32] we take on the band-offset ratio to be equal to 70/30. The assumption that the confinement potential depends on the indium concentration distribution allows us—at least partially—to take into account the strain present in the nanostructure. The indium concentration is assumed to vary in a quantum ring as follows:

$$X(\rho) = X_0\left[\mathrm{e}^{-(\rho/R_o)^2} - C\mathrm{e}^{-(\rho/R_i)^2}\right] \tag{3}$$

where ρ is the distance measured from the centre of the nanostructure, R_o and R_i are the outer and inner radius of the quantum ring, respectively, X_0 describes the maximal concentration of indium in the quantum dot, and parameter $C \in (0, 1)$ is responsible for the depletion of the indium concentration near the centre of the quantum ring. The second term in equation (3) enables us to introduce the repulsive core potential for electrons and holes via formulas (1) and (2). In the following, parameter C will be referred to as 'strength of the repulsive core'. In this paper, we mainly concentrate on the dependence of the exciton energy spectrum on parameter C. The nanostructure, for which $C = 0$, will be referred to as a 'Gaussian quantum dot' and that with the repulsive core, i.e. $C > 0$, will be called a 'quantum ring'. The shape of the confinement potential for different values of C is drawn in figure 1.

The cylindrical symmetry assumed in the indium distribution function (3) is well justified by the AFM images of the nanostructures [13]. The adopted modelling of the confinement potential (equations (1)–(3)) allows for description of the ring-like potential for both the electrons and holes with use of a minimal set of parameters. The model confinement potential introduced by equations (1)–(3) possesses a finite depth and range, and smooth boundaries.

These are just the properties of the realistic confinement in self-assembled quantum dots. Therefore, the present approach provides an essential development in a description of InGaAs quantum rings with respect to the previous models [15–17,20–23], which use the confinement potentials with one-dimensional [22,23], step-like, [15–17,21] and parabolic [20,21] profiles.

We apply the following effective mass Hamiltonian for the exciton:

$$H = -\frac{\hbar^2}{2m_e}\nabla_e^2 - \frac{\hbar^2}{2m_h}\nabla_h^2 - \frac{e^2}{4\pi\varepsilon_0\varepsilon_s\rho_{eh}} + V_e(\rho_e) + V_h(\rho_h) \tag{4}$$

where ρ_e and ρ_h are the distances of the electron and the hole from the centre of the nanostructure, ρ_{eh} is the interparticle distance, m_e and m_h are the electron and hole effective band masses, and ε_s is the static dielectric constant of the quantum-dot (quantum-ring) material. Throughout this paper, we put zero on the energy scale at the energy of the continuum threshold for the exciton, which corresponds to the minimum energy of the unbound electron–hole pair with both the charge carriers outside the range of the confinement potential.

In order to calculate the energy spectrum of the exciton confined in the quantum ring, we propose the following variational trial wavefunction:

$$\varphi(\boldsymbol{r}_e, \boldsymbol{r}_h) = \sum_{i,j,k,l=0}^{i+j,k+l\leqslant K} \sum_{n=1}^{n\leqslant L} c_{ijkln} x_e^i y_e^j x_h^k y_h^l \exp(-\alpha_e\rho_e^2 - \alpha_h\rho_h^2 - \beta_n\rho_{eh}^2) \tag{5}$$

where c_{ijkln} are the linear variational parameters, α_e, α_h and β_n are the nonlinear variational parameters. Parameters β_n, which are responsible for the relative electron–hole localization, are taken according to a geometrical progression, i.e. $\beta_n = \beta_1 q^n$ with $q = 10$. The optimal values of the linear variational parameters c_{ijkln} for the subsequent states are obtained by the diagonalization of the generalized eigenvalue problem defined by the Hamiltonian and overlap matrices for basis (5) with given values of α_e, α_h, and β_1. The optimal values of these parameters are obtained by a minimization of the ground state energy upper bound. The actual values of parameters c_{ijkln}, obtained from the diagonalization procedure enable us to construct the eigenstates of the total angular momentum. We have performed the calculations with the following upper limits on the summations in equation (5): $K = 6$ and $L = 3$, which—as we shall show later on—guarantee that the energy estimates for the problems discussed in this paper are determined with a precision of $\sim$1 meV. In equation (5), the inclusion of the high-order powers of x and y coordinates of both the carriers not only improves the description of the angular interparticle correlation, but also enables us to perform the calculations for the ring-like structures with a strong repulsive potential at the centre of the dot. The in-plane correlation of the electron–hole motion can be neglected [29] in the first approximation if the lateral size of the quantum dot is not too large. However, in the nanostructures, which are large in comparison with the bulk exciton radius, for example, in InGaAs quantum rings [12–14], this correlation cannot be neglected. In order to describe the effect of the electron–hole correlation, we had to include the explicit dependence of a trial wavefunction (5) on the interparticle distance. We have checked that the configuration-interaction approach, in which this dependence is not explicitly included in the wavefunction, applied to the excitons in large quantum dots, is very slowly convergent.

3. Results and discussion

In order to check the flexibility of the proposed trial wavefunction (5), we have performed the test calculations of the energy spectrum and the oscillator strengths for an exciton confined in a two-dimensional harmonic potential and compared the present results with those obtained by Halonen *et al* [33]. We have applied the same values for the material parameters ($\varepsilon_s = 13.1$,

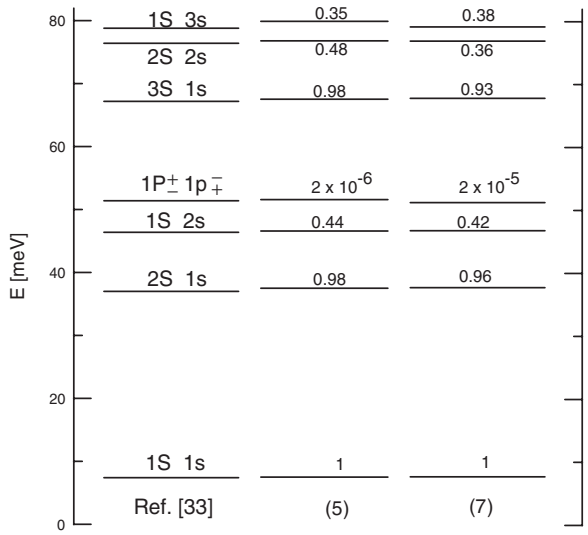

Figure 2. Calculated energy levels of the lowest-energy states of an exciton confined in a two-dimensional harmonic oscillator potential obtained with the use of trial wavefunctions (5) (central plot) and (7) (right plot) compared with the results of [33] (left plot). The states are labelled according to the spectroscopic notation for the centre-of-mass motion (first symbols with capital letters) and relative motion (second symbols with small letters). In the central and right plots, the numbers above the levels are the relative oscillator strengths calculated with respect to the oscillator strength of the ground state.

$m_e = 0.067m_0$, $m_h = 0.09m_0$, where m_0 is the electron rest mass) and the confinement potential with the same oscillator energy for the electron and the hole ($\hbar\omega_e = \hbar\omega_h = 15$ meV) as given therein [33]. The comparison of the results is given in figure 2, which displays the lowest-energy levels of the given symmetry. In figure 2, the states of the centre-of-mass (relative) motion are labelled by the capital (small) letters as follows: S and P (s and p) correspond to the angular-momentum quantum numbers 0 and 1, respectively, and for the p states the sign of the z component of the angular momentum is given.

In this paper, we consider only the exciton states of s angular symmetry corresponding to zero total angular momentum. The probability of radiative interband transition from the initial exciton state described by the wavefunction $\varphi(\boldsymbol{r}_e, \boldsymbol{r}_h)$ is proportional to the relative oscillator strength given by

$$I = \left| \int \mathrm{d}^2\boldsymbol{r}_e \, \mathrm{d}^2\boldsymbol{r}_h \, \varphi(\boldsymbol{r}_e, \boldsymbol{r}_h)\delta(\boldsymbol{r}_e - \boldsymbol{r}_h) \right|^2. \tag{6}$$

According to equation (6), only the s states can be 'optically active' i.e. are characterized by the non-zero oscillator strength for radiative recombination.

Basis (5) allows for a construction of states of the non-zero angular momentum. Possible numerical errors might result in an appearance of artificial states a which are not angular momentum eigenstates and possess non-zero oscillator strengths. In order to exclude this possibility the results obtained with the trial wavefunction (5) have been additionally tested with the use of a different variational wavefunction which allows for the construction of the s symmetry states only. Namely, we have performed test calculations for the exciton states of

zero total angular-momentum using the following variational wavefunction:

$$\varphi_s(\rho_e, \rho_h, \rho_{eh}) = \sum_{i,j,k=1}^{i,k,l \leqslant N} d_{ijk} \exp(-\gamma_i^e \rho_e^2 - \gamma_j^h \rho_h^2 - \gamma_k^{eh} \rho_{eh}^2). \tag{7}$$

The nonlinear variational parameters are taken as $\gamma_l^{e,h,eh} = \gamma_1^{e,h,eh} q^l$, where $q = 4$. In this paper, we present the results obtained with the use of trial wavefunction (7) with $N = 6$. The left plot in figure 2 shows the energy levels obtained by Halonen *et al* [33] from a diagonalization of the exciton Hamiltonian in the basis constructed from the products of the eigenstates of the relative and centre-of-mass Hamiltonians. In the central and right part of figure 2, we have plotted the present results obtained with the use of bases (5) and (7), respectively. In these parts of figure 2, the numbers above the horizontal lines show the estimated probabilities of the radiative transitions for the corresponding states. We see that the differences between the present and previous [33] energy estimates are negligibly small as compared with the energy-level separations (the largest deviation is equal to 1.1 meV for the highest excited state considered). The energy estimates as well as the oscillator strengths obtained with both the trial wavefunctions (equations (5) and (7)) agree with each other. The oscillator strengths calculated by the present method are also in a good agreement with the results presented graphically in figure 8 of [33]. These results provide the arguments for the reliability of the present approach.

In the case of the equal oscillator energies for electron and the hole (like that discussed above) the problem of the confined exciton can be separated into the relative and centre-of-mass coordinates. For the separable problem the oscillator strength depends on the relative-motion state only. Thus, the oscillator strengths for the states 1S 1s, 2S 1s, and 3S 1s should be equal to each other. Due to the same reasons, the states 1S 2s and 2S 2s should have the same oscillator strengths, and the oscillator strength for the $1P^{\pm}$ $1p^{\pm}$ states should vanish. We see from figure 2 that the results of the present calculations are close to the exact results.

Bases (5) and (7) have also been applied to the exciton confined in the Gaussian quantum dot. For the InGaAs self-assembled quantum dots [11] we have used the following values [29] of the confinement-potential parameters: $C = 0$, $X_0 = 0.66$ and $R_o = 25$ nm, and the material parameters of the quantum dot: static dielectric constant $\varepsilon_s = 12.5$ for the InGaAs, and the effective masses: $m_e = 0.045m_0$ and $m_h = 0.45m_0$, taken as the average values of the BenDaniel–Duke [34] approach used in [29]. The energies of the four lowest-energy optically active states and the corresponding oscillator strengths are listed in table 1. We see that the energy levels are clearly separated and that the energy separations get smaller for the higher-energy states. The results are in a good qualitative agreement with the experimental data [11] and the results of our previous three-dimensional calculations [29], in which the in-plane correlations were neglected. A good agreement obtained for the energy eigenvalues as well as oscillator strength (cf figure 2 and table 1) with the use of variational wavefunctions (5) and (7) supports the reliability of the present results.

Table 1 shows that the oscillator strength for the third excited state is larger than that for the ground state. This interesting feature deserves a further study. For the commonly studied case of parabolic confinement, the Hamiltonian of the exciton can be expressed [33] as the sum of three operators. The first operator depends on the relative position vector $\boldsymbol{r} = \boldsymbol{r}_{eh}$, the second on the centre-of-mass vector $\boldsymbol{R} = \boldsymbol{R}_{CM}$, and third is the cross term $m_e m_h/(m_e m_h)(\omega_e^2 - \omega_h^2)\boldsymbol{R}\cdot\boldsymbol{r}$. In the strictly separable case, the oscillator strength depends on the relative-motion state only and takes on the largest value for the ground state of the relative motion (cf figure 2). In the presence of the large cross term the relative and centre-of-mass motions are strongly coupled and cannot be separated even in an approximate manner. In this case, the states cannot be described by the centre-of-mass and relative-motion quantum numbers. The coupling between the centre-of-mass and relative motion is strong if the oscillator energy of one particle is much

Table 1. Lowest-energy levels (E_ν) and relative oscillator strengths (I) for the radiative transitions from the corresponding quantum states of an exciton confined in a Gaussian quantum dot. The second (E_ν) and third (I) columns show the values obtained with variational basis (5). The values given in the fourth (E^s_ν) and fifth (I^s) columns have been obtained with basis (7). The parameters of the confinement potential correspond to the InGaAs self-assembled quantum dots. Energy is expressed in meV and oscillator strengths in arbitrary units.

ν	E_ν	I	E^s_ν	I^s
0	−705.35	1	−705.38	1
1	−676.15	0.53	−676.13	0.54
2	−650.28	0.08	−649.56	0.11
3	−633.53	1.38	−632.23	1.40

larger than that of the other, i.e. $\omega_e \gg \omega_h$ or $\omega_e \ll \omega_h$, and if these energies are at least of the order of the Coulomb interaction energy. In the case of strong coupling an excited state can possess a larger oscillator strength than the ground state which occurs for InGaAs self-assembled quantum dots (cf table 1). In this case the oscillator energies are $\hbar\omega_h \simeq 10$ meV, $\hbar\omega_e \simeq 50$ meV, and the energy of the Coulomb interaction in the ground state is ∼35 meV. We have verified that this effect is not related with the Gaussian shape of the confinement potential and is also obtained for the harmonic confinement.

In order to illustrate the influence of the cross-term on the exciton wavefunction we have calculated the integral

$$P(r) = \int \mathrm{d}^2\boldsymbol{R}\,|\varphi(\boldsymbol{R}, \boldsymbol{r})|^2. \tag{8}$$

The integral P can be interpreted as the probability density of finding the electron–hole pair separated by r. In the case of a strict separation of the centre-of-mass and relative-motion Hamiltonians, probability density P is the same for all the states corresponding to the same relative-motion quantum state. In figures 3(a) and (b), integral P is plotted for the nonseparable problem of the Gaussian quantum dot with $C = 0$ for (a) $R_o = 25$ nm, which corresponds to the real self-assembled quantum dots and (b) $R_o = 200$ nm, i.e. the nearly free exciton (weak confinement) in which the cross term is small (all the other parameters are kept the same as in table 1). The dashed curve in figure 3(a) corresponds to the state with the oscillator strength larger than that for the ground state (cf table 1). In the nearly separable case (figure 3(b)), the oscillator strength is the largest for the ground state and gets smaller for the excited states. Figure 3(b) shows that the four lowest-energy states (solid curves) correspond approximately to the ground state of the relative motion. The relative probability density for the fifth state (dashed curve in figure 3(b)) contains a considerable admixture of the excited relative-motion state. The results of figures 3(a) and (b) show that the classification of the quantum states according to the centre-of-mass and relative-motion quantization is not justified for the parameters which correspond to real InGaAs self-assembled quantum dots. Moreover, one can expect that the presence of the repulsive core in the quantum ring potential would additionally spoil the picture of the separable centre-of-mass and relative motions.

We have studied the size of the variational basis (5) which is needed to a description of the one-particle electron and hole states in the quantum ring. We have used the geometrical parameters of the confinement potential corresponding to the InGaAs self-assembled quantum rings [13], i.e. $R_o = 50$ nm, $R_i = 10$ nm, and the material parameters for GaAs: $m_e = 0.067m_0$, $m_h = 0.377m_0$, and $\varepsilon_s = 13.1$. Moreover, we have set $X_0 = 0.5$, which is equivalent to the assumption that effective indium concentration in the Gaussian quantum dot without the repulsive core is 50%. The above values of the material parameters are used

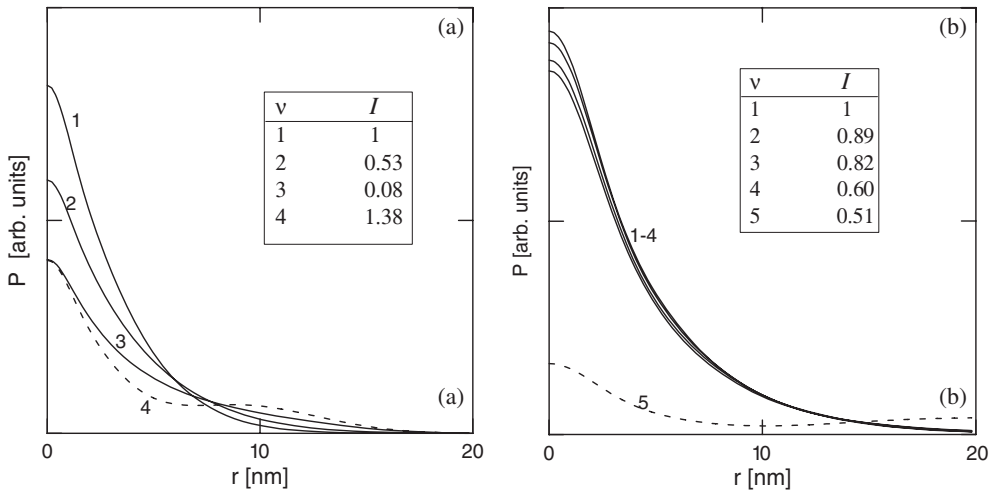

Figure 3. Integral P (equation (8)) as a function of relative electron–hole distance r for the subsequent states (labelled by the integers) of the exciton confined in the Gaussian quantum dot with (a) $R_o = 25$ nm and (b) $R_o = 200$ nm. The insets show the values of the oscillator strength corresponding to the labelled states.

Table 2. Energy estimates for the three lowest-energy levels of an electron confined in a quantum ring with $C = 1$ for different K, i.e. the maximal value of the sum of exponents of the x_e and y_e variables in the trial wavefunction (equation (5)) for $R_o = 50$ nm, $R_i = 10$ nm, $X_0 = 0.5$, and $C = 1$. Energy is expressed in meV.

K	E_0	E_1	E_2
2	−293.32	−287.16	−161.68
4	−303.93	−297.75	−277.80
6	−305.24	−298.80	−280.92
8	−305.30	−298.82	−281.18
10	−305.31	−298.82	−281.18

throughout the rest of this paper. The calculated lowest-energy levels of an electron confined in a quantum ring ($C = 1$) are listed in table 2 as functions of K (the upper bound on summation in wavefunction (5)). We see that the convergence of the variational estimates is achieved for $K = 6$ with a precision better than 1 meV. Therefore, in the following, we take on $K = 6$ in wavefunction (5). The convergence is faster for the hole, which is much heavier than the electron. The trial wavefunction proposed in equation (7) yields the results of similar accuracy for $C \lesssim 0.3$. However, for $C > 0.3$ the energy estimates obtained with trial wavefunction (7) become significantly worse. The inclusion of the high order powers in the basis (5) describes the effect of the repulsive core much better than the superposition of Gaussian functions (equation (7)). All the results presented in the following part of the paper have been obtained with trial wavefunction (5).

Figure 4 shows the calculated exciton ground state energy as a function of the strength of the repulsive core (C). If the central repulsive core is introduced into the nanostructure, the potential-well depth decreases and the space occupied by the carriers shrinks. This leads to the growth of the exciton ground state energy. The inset in figure 4 shows the calculated oscillator strength for the interband radiative transitions to/from the ground state as a function of parameter C. We see that the oscillator strength is 4–5 times larger for the quantum ring

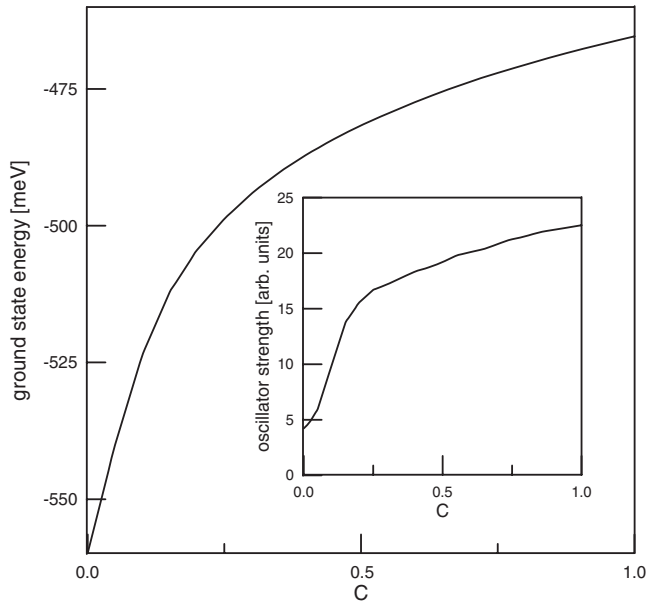

Figure 4. Ground state energy of the exciton confined in the quantum ring as a function of strength C of the repulsive core. The inset shows the oscillator strength for the radiative interband transition from the ground state.

($C = 1$) than for the Gaussian quantum dot ($C = 0$). This growth of the oscillator strength for the ground state can be explained if we consider the limit case of the ground state of the exciton in a one-dimensional quantum ring [22, 23], i.e. a ring with zero width. In this case, the electron wavefunction exhibits a delta-like localization at the hole position. Let us consider the more realistic, two-dimensional model of a quantum ring of nonzero width. If the repulsive core (C) is increased the width of the ring decreases and the model nanostructure approaches the one-dimensional limit. Therefore, introduction of the repulsive core in the potential causes that the charge carriers in the ground state become localized closer to each other, which—according to equation (6)—leads to the increase of the oscillator strength.

In figure 5, we have plotted the energy shifts of the six lowest optically active excited states calculated with respect to the ground state energy. In figure 5, the centres of the full circles are placed at the positions, which show the calculated energy shifts, and the areas of these circles correspond to the relative values of the oscillator strengths calculated with respect to the radiative transition probability for the ground state. In the Gaussian quantum dot ($C = 0$), the exciton in the ground state is more strongly localized near the centre of the dot than in the excited states. Therefore, the repulsive core introduced at the centre of the nanostructure makes the ground state energy grow faster than the energy of the excited states. As a result the energy shifts decrease for $C \in (0, 0.15)$. The situation changes if $C > 0.15$. In this case the energies of the excited states start to grow faster than the ground state energy. So, the corresponding energy shifts increase after passing through a minimum. This is due to the fact that the oscillations of excited-state wavefunctions become energetically more expensive when the width of the ring shrinks with increasing strength of the repulsive core.

In the case of the Gaussian quantum dot ($C = 0$), the oscillator strengths for the excited states and the ground state are of the same order. As the strength C of the repulsive core increases, the radiative transition probabilities for the excited states become smaller compared

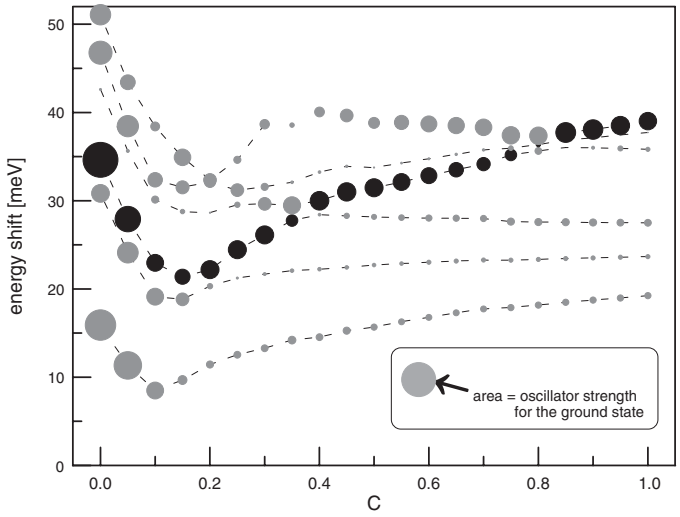

Figure 5. Energy shifts for the six lowest-energy optically active excited states of the exciton calculated with respect to the exciton ground state energy as functions of strength C of the repulsive core. The areas of the circles correspond to the relative value of the oscillator strengths calculated with respect to the oscillator strength for the ground state. The energy level of the state with the relatively large oscillator strength is marked by the black circles (see the discussion in the text). The dashed curves are guides to an eye.

with the value for the ground state. Finally, for $C = 1$, the values of the oscillator strengths for the five lowest-energy excited states are $\sim$8 times smaller that the oscillator strength for the ground state. The exciton spectrum as a function of C (cf figure 5) exhibits several anti-crossings between the energy levels (all the optically active states are of the same symmetry corresponding to the zero total angular momentum). As the result of the anti-crossing the exciton state with a distinctly larger oscillator strength is pushed up in the exciton spectrum. The results for this state are marked by the black circles in figure 5. We note that the position of this intensive exciton line changes with increasing C, e.g. the black-marked circles correspond to the third exciton line for $C \lesssim 0.4$, the fourth line for $\sim 0.4 < C \lesssim 0.8$, and the fifth and sixth line for $C \gtrsim 0.8$.

In order to get some insight into the characteristic features of excitons confined in quantum rings, i.e. the changes of the relative oscillator strengths for the ground and excited states as well as the large blue-shift of the energy level, which corresponds to the state with the large oscillator strength, we have studied the evolution of the exciton wavefunctions as the confinement potential is changed from the Gaussian quantum dot to the quantum ring. In figures 6 and 7, we have plotted the contours of exciton wavefunction $\varphi(x_e, y_e, x_h, y_h)$ on the x_h–y_h plane with the electron position fixed near the minimum of the confinement potential. This choice of the way of presentation enables us to illustrate both the effects of the repulsive core and the effect of correlated movement of the particles. A possible integration over the centre-of-mass coordinates would cause a loss of much of the information. Figures 6(a) and (b) show the plots for the ground state and the lowest-energy optically active excited state in the Gaussian quantum dot ($C = 0$). In figure 6, the electron is located at the position $x_e = 0$, $y_e = 2$ nm, which is marked by the intersection of the two perpendicular thin solid lines. Figures 7(a)–(e) show the wavefunction contours for the ground and the four lowest-energy optically active excited states for the quantum ring with $C = 0.4$ (the electron coordinates are

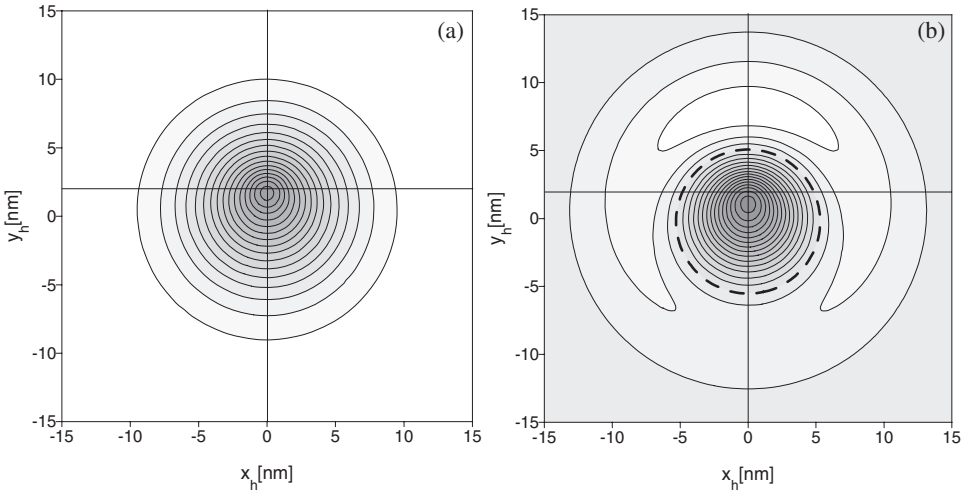

Figure 6. Contours of the wavefunctions in the x_h–y_h plane for the ground state (a) and the first optically active excited state (b) for the exciton confined in the Gaussian quantum dot ($C = 0$). The position of the electron is fixed at ($x_e = 0$, $y_e = 2$ nm), i.e. near the minimum of the confinement potential and marked by the intersection of the two thin solid lines. In panel (b), the thick dashed plot corresponds to the nodal line.

$x_e = 0$, $y_e = 15.5$ nm). The case of $C = 0.4$ corresponds to the anti-crossing of the third and fourth excited energy levels (cf figure 5). The qualitative properties of the wavefunctions of the ground state and the three optically active excited states remain the same for C up to 1.

The comparison of the ground state wavefunctions for the Gaussian quantum dot (figure 6(a)) and for the quantum ring (figure 7(a)) shows that—in the latter case—the hole is more strongly localized around the electron, which is connected with the additional in-plane confinement of the quantum ring. For the excited states the specific shape of the nodal lines, marked by the thick dashed curves in figures 6(b) and 7(b) through 7(e), results from the orthogonality conditions. We see that—for the Gaussian quantum dot (figure 6(b))—the orthogonality does not prevent the hole from penetrating into the region, in which the electron is localized. For this reason the oscillator strengths for both the ground and excited states of the exciton in the Gaussian quantum dot are of the same order of magnitude.

Let us discuss the shape of the excited-state wavefunctions for the exciton in the quantum ring (figures 7(b)–(e)). In the lowest-energy optically active excited state (figure 7(b)) the electron is localized close to the nodal line of the hole wavefunction, which is the reason of the small oscillator strength for this state (cf figure 5). We note that the wavefunction in figure 7(b) possesses two local extrema and changes the sign along the radius of the ring. This means that in the quantum rings of the finite width, which correspond to the fabricated nanostructures [12–14], the lowest-energy optically active excited state cannot be described in the framework of the strictly one-dimensional model [22, 23]. For the two subsequent excited states (figures 7(c), (d)) the local extrema of the wavefunctions are placed on the circumference of the ring. These wavefunctions exhibit local extrema at the electron position, but the major part of the hole wavefunction is pushed away to the opposite side of the quantum ring, which explains why the corresponding oscillator strengths are small. The wavefunction of the fourth excited state (figure 7(e)) is strongly localized around the electron position; therefore, the corresponding oscillator strength is relatively large. The energy level associated with this state is marked by the black circles in figure 5. For large C the blue-shift of this energy level

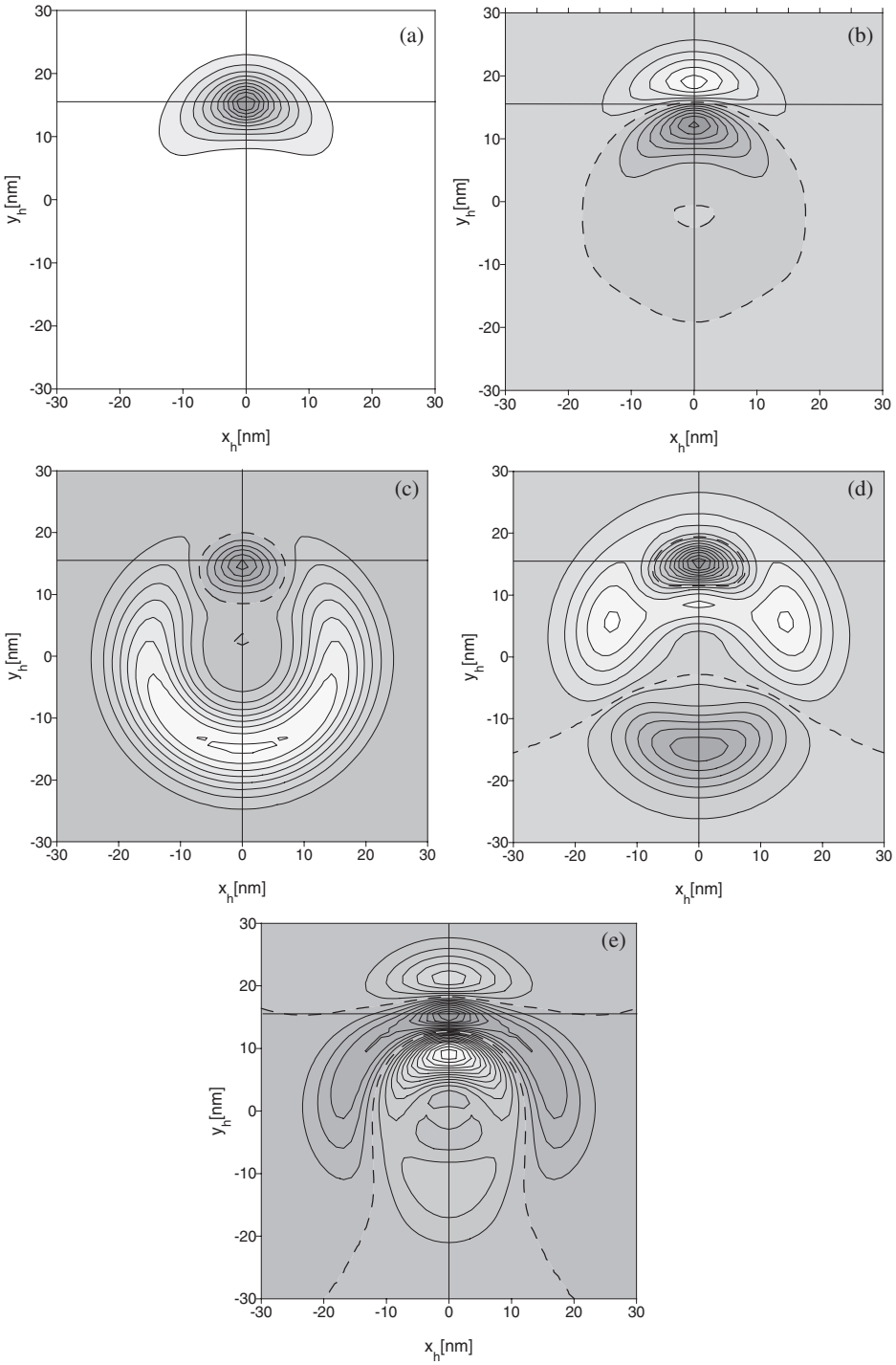

Figure 7. Contours of the wavefunctions in the x_h–y_h plane for the ground state (a) and the four lowest-energy optically active excited states (b)–(e) of the exciton confined in the Gaussian quantum ring with $C = 0.4$. The position of the electron is fixed at the minimum of the confinement potential ($x_e = 0$, $y_e = 15.5$ nm) and marked by the intersection of the thin solid curves. The thick dashed curves correspond to the nodal curves.

is considerably larger than those of the neighbouring levels. The wavefunction shown in figure 7(e) changes sign along the radius of the ring, which explains the fact that the change of the quantum-ring width affects this energy level more strongly than other energy levels.

4. Conclusions

The results of figures 6 and 7 allow us to explain the characteristic properties of the oscillator strengths for the interband radiative transitions from the ground and excited states of excitons confined in quantum dots and quantum rings. These properties can be observed when the shape of the confinement potential changes from the Gaussian quantum dot to the quantum ring. In the exciton ground state, the charge carriers are more strongly localized near each other in the quantum ring than in the Gaussian quantum dot, which causes the increase of the oscillator strength in the quantum ring with respect to that in the Gaussian quantum dot. In the excited states, the orthogonality of the wavefunctions in the reduced space of the quantum ring forces the charge carriers to avoid each other, which is the reason for the decrease of the corresponding oscillator strengths. The excited state with the large oscillator strength is described by the wavefunction that exhibits the oscillations along the radial direction. The energy level corresponding to this state is more strongly blue-shifted than the energy levels of the states with smaller oscillator strengths, which leads to characteristic level anti-crossings displayed in figure 5. In consequence of these anti-crossings, the state with the larger oscillator strength appears in the higher-energy part of the exciton spectrum.

The present explanation of the change of the relative values of the oscillator strength for the ground and excited exciton states confirms the conclusions drawn in [20] and contradicts those presented in [21]. Based on the present results, we suggest that the exciton spectrum and—in particular—the relative intensities of optical lines can be used in order to detect the presence of the repulsive core in the centre of a quantum dot. Moreover, the discussed strong blue-shift of the line with the large oscillator strength may be useful in determining the strength of the repulsive core from the relative position of the strong-intensity line with respect to the weaker lines.

5. Summary

We have presented the results of the calculations for the exciton confined in the quantum dot with the tuned strength of the repulsive core. The use of the model confinement potential with the tunable repulsive core enables us to investigate the evolution of the exciton spectrum and the oscillator strengths for the subsequent exciton states when the character of the potential changes from the Gaussian quantum dot to the quantum ring. We have applied the variational wavefunction, that accurately describes both the one-particle confinement effects and the electron–hole correlated motion. We have shown that—with increasing strength of the repulsive core—the probability of radiative transitions from the exciton ground state strongly increases at the expense of the probabilities of transitions from the excited states. We have explained this effect by the character of the quantum-ring confinement potential, in which the charge carriers in the ground state are more strongly localized at each other than in the Gaussian quantum dot. For the exciton ground state with such properties the orthogonality of the excited-state wavefunctions leads to the pronounced separation of both the charge carriers, which appears in the lowest-energy optically active excited states. This paper settles the controversy between the interpretation of the results of [20] and [21] in favour of [20]. Moreover, we have shown that the excited state with the larger oscillator strength is more strongly blue-shifted by

the repulsive core than the states corresponding to weaker optical lines. We have suggested that the presence as well as the strength of the repulsive core in the quantum dot can be determined with use of the relative intensities of the exciton photoluminescence lines.

Acknowledgment

One of the authors (BS) gratefully acknowledges the financial support from the Foundation for Polish Science (FNP).

References

[1] For a review, see Chakraborty T 1992 *Comments Condens. Matter Phys.* **16** 35
Kastner M A 1993 *Phys. Today* **46** 24
Kastner M A 1996 *Comments Condens. Matter Phys.* **17** 349
Jacak L, Hawrylak P and Wójs A 1998 *Quantum Dots* (Berlin: Springer)
[2] Maksym P A and Chakraborty T 1990 *Phys. Rev. Lett.* **65** 108
[3] Bednarek S, Szafran B and Adamowski J 1999 *Phys. Rev.* B **59** 13 036
[4] Warburton R J, Dűrr C S, Karrai K, Kotthaus J P, Medeiros-Ribeiro G and Petroff P M 1997 *Phys. Rev. Lett.* **79** 5282
[5] Grundmann M, Stier O and Bimberg D 1995 *Phys. Rev.* B **52** 11 969
[6] Szafran B, Adamowski J and Bednarek S 2000 *Phys. Rev.* B **61** 1971
[7] Bayer M, Stern O, Hawrylak P, Fafard S and Forchel A 2000 *Nature* **405** 923
[8] Williamson A J, Wang L W and Zunger A 2000 *Phys. Rev.* B **62** 12 963
[9] Franceschetti A, Fu H, Wang L W and Zunger A 1999 *Phys. Rev.* B **60** 1819
[10] Wójs A and Hawrylak P 1996 *Phys. Rev.* B **53** 10 841
[11] Fafard S, Spanner M, McCaffrey J P and Wasilewski Z R 2000 *Appl. Phys. Lett.* **76** 2268
[12] Petterson H, Warburton R J, Lorke A, Karrai K, Kotthaus J P, Garcia J M and Pettrof P M 2000 *Physica* E **6** 510
[13] Lorke A, Luyken R J, Govorov A O, Kotthaus J P, Garcia J M and Petroff P M 2000 *Phys. Rev. Lett.* **84** 2223
[14] Warburton R J, Schäflein C, Haft D, Bickel F, Lorke A, Karrai K, Garcia J M, Schoenfeld W and Petroff P M 2000 *Nature* **405** 926
[15] Bruno-Alfonso A and Latgé A 2000 *Phys. Rev.* B **61** 15 887
[16] Barticevic Z, Pacheco M and Latgé A 2000 *Phys. Rev.* B **62** 6963
[17] Varga K, Navratil P, Usukura J and Suzuki Y 2001 *Phys. Rev.* B **63** 205308
[18] Margulis V A, Shorokhov A V and Trushin M P 2001 *Physica* E **10** 518
[19] Puente A and Serra L 2001 *Phys. Rev.* B **63** 125334
[20] Hu H, Zhu J-L, Li D-J and Xiong J-J 2001 *Phys. Rev.* B **63** 195307
[21] Song J and Ulloa S E 2001 *Phys. Rev.* B **63** 125302
[22] Chaplik A 1995 *JETP Lett.* **62** 900
[23] Römer R A and Raikh M E 2000 *Phys. Rev.* B **62** 7045
[24] Adolph B, Glutsch S and Bechstedt F 1993 *Phys. Rev.* B **48** 15 077
[25] Glutsch S, Chemla D S and Bechstedt F 1996 *Phys. Rev.* B **54** 11 592
[26] Stier O, Grundman M and Bimberg D 1999 *Phys. Rev.* B **59** 5688
[27] Hu Y Z, Giessen H, Peyhambarian N and Koch S W 1996 *Phys. Rev.* B **53** 4814
[28] Adamowski J, Sobkowicz M, Szafran B and Bednarek S 2000 *Phys. Rev.* B **62** 4234
[29] Szafran B, Bednarek S and Adamowski J 2001 *Phys. Rev.* B **64** 125301
[30] Raymond S, Guo X, Merz J L, Fafard S and Spanner M 1999 *Phys. Rev.* B **59** 7624
[31] Siverns P D, Malik S, McPherson G, Childs D, Roberts C, Murray R, Joyce B A and Davock H 1998 *Phys. Rev.* **58** R10 127
[32] Colombelli R, Piazza V, Badolato A, Lazzarino M, Beltram F, Schoenfeld W and Petroff P 2000 *Appl. Phys. Lett.* **76** 1146
[33] Halonen V, Chakraborty T and Pietiläinen P 1992 *Phys. Rev.* B **45** 5980
[34] BenDaniel D J and Duke C B 1966 *Phys. Rev.* **152** 683